ACCSCIENCE PUBLISHING

International Journal of AI for Materials and Design

ORIGINAL RESEARCH ARTICLE

Machine learning and exploratory data analysis for predicting tensile and thermal responses in friction stir spot welding

Sajad N. Alasadi and Raheem Al-Sabur*

Department of Mechanical Engineering College, University of Basrah, Basrah, Iraq

Abstract

Friction stir spot welding (FSSW) has gained increasing attention over the last decade due to its promising performance compared to conventional joining methods for similar metals. However, the thermal and tensile responses in this process are highly nonlinear. This study aims to explore the thermal and tensile performance of aluminum joints welded by FSSW using an innovative method based on exploratory data analysis (EDA), followed by several machine learning (ML) approaches. The welding parameters investigated in this study were tool rotational speed, dwelling time, and aluminum sheet thickness. The ML methods included linear and nonlinear regression models for welded joints at different welding parameters. We evaluated Bayesian ridge, elastic-net, support vector regression (SVR), random forest, polynomial regression (nonlinear), and robust regression. The random forest algorithm provided accurate predictions for lap-shear fracture load (R^2 = 0.96, mean squared error [MSE] = 0.01, and mean absolute error [MAE] = 0.07) in tensile performance, whereas the elastic net performed worst. Model-to-model differences were smaller for thermal performance, with the random forest model yielding the most accurate predictions (R^2 = 0.97, MSE = 26.51, and MAE = 3.86) while the SVR yielded the least accurate predictions. The study indicated that using EDA to address anomalies in welding conditions provides valuable insights into the best ML methods for predicting the thermal and mechanical performance of welding joints.

Keywords: Friction stir spot welding; Machine learning; Exploratory data analysis; Tensile performance; Thermal performance

***Corresponding author:**
Raheem Al-Sabur
(raheem.musawel@uobasrah.edu.iq)

Citation: Alasadi SN, Al-Sabur R. Machine learning and exploratory data analysis for predicting tensile and thermal responses in friction stir spot welding. *Int J AI Mater Design*. 2025;2(4):37-51.
doi: 10.36922/IJAMD025360032

Received: September 1, 2025

Revised: December 15, 2025

Accepted: December 16, 2025

Published online: December 30, 2025

1. Introduction

Over the past decade, the use of solid-state welding has grown significantly, primarily due to its ability to generate heat below the melting point of the base metals, thereby minimizing defects in the weld zone and the surrounding material.[1,2] A notable trend during this period is the dominance of friction stir welding (FSW) in academic research compared to other solid-state welding techniques.[3] In addition, FSW is classified as an eco-friendly welding method; it does not produce any fumes or spatter, is less energy-intensive, and does not cause significant changes in the microstructure.[4,5] Initially, FSW was limited to aluminum alloys and gradually expanded to include other alloys, such as magnesium, copper, and even steel. Further developments have given FSW a significant advantage over conventional welding, particularly in its ability to weld dissimilar metals, including those with substantial differences in melting points.[6] Furthermore, FSW has expanded to include the welding of polymeric materials and composites.[7]

The FSW mechanism differs significantly from most welding processes, as the welding tool is reusable. The welding tool is typically made of tool steel or cemented carbide, selected for high hardness and wear resistance.[8,9] A lathe process typically forms the tool, consisting of two interconnected parts. The first part is cylindrical, has a suitable length and diameter, and is referred to as the shoulder. The other part is shorter and narrower, can be tapered, and is called the pin.[10] The welding tool is securely attached to the FSW machine, typically a specialized unit designed for this process. Alternatively, computer numerical control machines can be adapted for FSW. For friction stir spot welding (FSSW), milling machines or even punching machines may also be used.[11,12] The two plates to be welded are firmly clamped together, usually in a butt joint configuration, though lap joints are also possible.[13] The process begins when the welding tool is lowered vertically onto the area to be welded at a specific rotational speed, depending on the type of metal to be welded.[14,15] The tool penetrates the right plate and a portion of the left plate due to frictional heat. Once the material beneath the shoulder becomes sufficiently plasticized, the welding tool begins a transverse movement along the weld line in addition to its rotational movement. This process yields a satisfactory weld between the two plates, with fewer defects, while generating flash metal on both ends of the weld line.[16] Upon reaching the endpoint of the weld, the tool rises, leaving a keyhole. FSSW is a special case of FSW in which spot welding is performed using the heat generated from the tool's rotational motion, and the transverse velocity is reduced, as shown in Figure 1.

Since John laid the foundation for exploratory data analysis (EDA),[17] the EDA approach has been steadily developed across numerous engineering applications,[18] although its use has also been limited to some welding problems.[19] The EDA approach begins by examining how the variables in the problem are distributed. EDA typically begins by examining the distributions of the variables of interest. In FSSW studies, EDA is primarily used to identify outliers and to explore relationships among welding parameters.[20] EDA therefore provides an initial basis for selecting appropriate models and interpreting results. The histograms visualize how key process parameters—such as material thickness, tool rotational speed, and dwell time—are distributed across the data.

Machine learning (ML) is a branch of artificial intelligence that has gained significant traction recently. ML focuses on developing algorithms and statistical models that enable computer systems to learn patterns and make decisions based on experimental data without requiring explicit programming for each task.[21,22] Welding has similarly benefited from those advances and is now widely applied in techniques such as arc welding,[23] laser welding,[24] ultrasonic welding,[25] and resistance spot welding.[26]

In the field of FSW and related welding methods, particularly FSSW, a substantial part of beneficial research has focused on the application of ML techniques. Studies have shown that ML can improve FSW process parameters by analyzing the relationship between input parameters and weld quality.[27] It can also accurately detect and classify defects by analyzing microstructure and classifying image properties.[28] It can also provide an in-depth description and better classification of the resulting weld joint.[29] Furthermore, it can predict weld quality by optimizing welding parameters and reducing defects, with greater potential to analyze the relationship between tool geometry and material properties and their association with weld joint quality.[30] In a previous study, artificial neural networks (ANNs) were used to predict stir zone hardness and determine optimal FSW parameters, particularly tool rotational speed and weld line velocity,

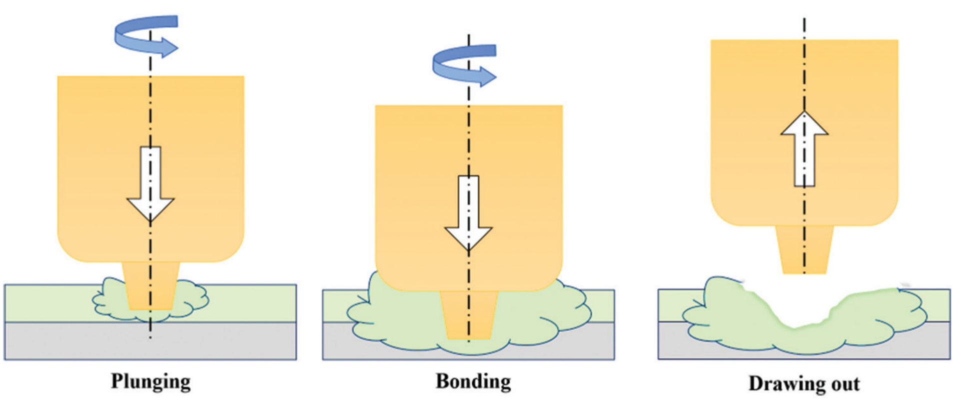

Figure 1. Process flow diagram of friction stir spot welding

in submerged 6061-T6 aluminum alloy.[31] ANNs have also shown remarkable performance in predicting wear rates during friction stir processing,[32] predicting tensile failure properties and fracture location of aluminum alloy 7075-T6 and duplex stainless steel,[33] and have been used to explore the thermal behavior and peak temperature in aluminum alloy.[34] In addition to ANNs, support vector machines (SVMs) have been utilized as ML tools in FSW and FSSW applications. For example, SVMs have been used for tensile-strength prediction[35] and for welding-process monitoring.[36] Several studies in FSSW and FSW focused on utilizing other ML tools, such as random forest.[37,38] Moreover, elastic-net,[39] ANN, and response surface methodology[40] were used in few FSW studies. Table 1 summarizes the most related studies.

FSSW is a solid-state welding process with a complex nonlinear nature. Therefore, understanding the tensile (lap-shear load) and thermal (maximum temperature) responses is complex. EDA and ML can help identify hidden correlations, while ML models effectively learn these nonlinear dependencies. ML, such as random forest, provides measures of feature importance that help understand parameter sensitivity. This study combines two approaches for an in-depth understanding of the prediction of the thermal and mechanical behavior of FSSW-welded aluminum alloys. EDA was employed alongside ML algorithms, marking a fundamental departure from traditional methods that rely solely on experimental approaches, simulations, or ML alone. In this study, we used EDA—including histograms, correlation matrices, and feature ranking—to uncover key patterns regarding shear stress and thermal behavior in the weld zone. We also conducted an in-depth comparison of several ML techniques, including random forest, elastic net, and Bayesian ridge, to determine the optimal welding conditions. Ultimately, this study offers a smart, scalable approach to optimizing the FSSW process, enabling easy prediction of the mechanical and thermal quality of the final joint.

2. Methodology

2.1. ML algorithms

ML applications have recently become evident across all sectors of industry. In this context, numerous studies

Table 1. Overall comparison between related previous studies

Process	Materials	ML algorithms	Key findings	References
FSW	AA2195	BPNN	Maximum tensile strength of 415 MPa with 92% prediction accuracy.	27
FSSW	Stainless steel and AA7075	SVM and ANN	The predicted tensile shear failure load is 4,967 N at 1,900 rpm.	33
FSP	AA6083 and AA8011	SVM, ANN, and RF	A 5.06 μm grain size is necessary to achieve the ultimate tensile strength.	28
FSW	Aluminum alloys	Multi-linear regression, K-nearest neighbor, RF, ANN, and SVM	ML is used to capture the relationship between the input and output FSW welding process	29
FSW	Aluminum alloys	Decision tree model, SVM, ANN, and CNN	An ML machine is used to achieve two key outcomes: enhanced quality assurance and improved automation	41
FSP	AA6061	ANN	Stir zone hardness prediction	31
FSW	Copper	ANN	Wear rate prediction in surface composites	32
FSW	AA7075	ANN	Peak temperature, torque, traverse force, bending stress, and maximum shear stress	34
FSW	AA5083 and AA5061	GPR and SVM	ML achieves 10.32% higher accuracy in tensile strength than regression methods	35
FSW	AA1100	discrete wavelet analysis and SVM	Using ML approaches to monitor and analyze FSW defect image classification	36
FSW	AA6061	SVM	FSW process parameter optimization	37
FSSW	AA7075	DTR, RF, and linear regression	The DTR can achieve better performance in the prediction of cross-tensile strength	38
FSW	Aluminum alloys	Bayesian ridge, k-nearest neighbor, RF, elastic-net, and SVM	The study highlights the potential of ML to forecast weld joint quality	39
	AA6061 and AZ31B	ANN and RSM	The accuracy of ANN's tensile strength prediction is better than RSM's	40

Abbreviations: ANNs: Artificial neural network; BPNN: Backpropagation neural network; CNN: Convolutional neural network; DTR: Decision tree regression; FSP: Friction stir processing; FSSW: Friction stir spot welding; FSW: Friction stir welding; ML: Machine learning; RF: Random forest; RSM: Response surface methodology; SVMs: Support vector machines.

have recommended adopting ML techniques in welding applications, specifically in two main categories: fusion welding and solid-state welding. Within the framework of fusion welding, Ramesh *et al.*[42] concluded that ML can be appropriate for detecting surface weld defects in electric arc welding, particularly shield metal arc welding. Tsai *et al.*[43] recommended ML as a suitable tool for optimizing laser welding parameters for lap joints. Based on these and other similar studies, this study aims to utilize and compare a range of ML tools to select optimal input parameters for achieving superior mechanical and thermal performance. Random forest, elastic net, Bayesian ridge, polynomial regression, and robust regression methods were used.

The random forest algorithm is considered an ensemble learning method and a supervised ML tool. It is a tree-based, non-parametric algorithm, with a primary purpose being regression or classification.[44,45] In welding, this technique has been used for several applications, including real-time defect detection in arc welding.[46,47] The random forest algorithm works by creating numerous decision trees, each trained on a random subset of the data (known as bootstrapping) and a random selection of features (referred to as feature bagging).[48] Each tree makes its prediction, and for regression tasks, the result is the average of all individual tree outputs. Elastic net regression is a regularized linear regression and a supervised ML approach. It is a parametric, linear model with Lasso and ridge regularizations. The primary purpose of elastic net regression is to enhance model generalization and address multicollinearity.[49] Several studies used elastic net regression in welding applications to assess quality in resistance spot welding.[50] The main purpose of using the Bayesian ridge regression is to incorporate prior distributions and provide uncertainty estimates. It is categorized as a probabilistic, linear regression, supervised ML tool.[51] Welding studies, such as predictive modeling of weld-bead geometry in wire-arc additive manufacturing, also employ Bayesian ridge regression.[52] Polynomial regression and robust regression are two supervised ML techniques used for predictive modeling, but they serve different purposes. Polynomial regression is a parametric approach that builds on linear regression by adding polynomial terms, such as squared or cubed predictors.[53] This enables it to capture curved, nonlinear relationships in the data. On the other hand, robust regression is a type of linear model built to handle messy datasets—especially those with outliers or heavy noise.[54] Unlike standard linear regression, it minimizes the impact of irregularities, making its predictions stable and reliable.

The Bayesian ridge was selected for its ability to produce probabilistic predictions, thereby enhancing the interpretability of uncertainty in tensile and thermal responses. Bayesian ridge provides stable estimates in the presence of multicollinearity, which can occur when process parameters (e.g., rotational speed and dwell time) influence responses in correlated ways. Elastic-net regression is suitable when only a subset of input features may strongly influence the output. It can lead to a better understanding of the influence of FSSW process parameters on the thermal and tensile behavior output. Random forest was selected for its ability to model complex nonlinear interactions among the FSSW parameters. The statistical basis of polynomial regression makes it an easy and suitable tool for interpretable nonlinear alternatives during the FSSW. The kernel functions of support vector regression (SVR) make it a powerful technique for learning nonlinear patterns without overfitting during the study of the FSSW process parameters and output responses. Robust regression reduces the influence of outliers and provides reliable predictions during the welding processes. In this study, Python (v3.15, Python Software Foundation, Netherlands) with Google Colab was used in EDA and ML prediction.

2.2. Experimental work

Aluminum alloy AA 6061 specimens of different thicknesses (1, 2, and 3 mm) and constant length and width (100 mm × 25 mm) were prepared in lap joint configurations and joined by FSSW in this study. A cylindrical welding tool with a diameter of 10 mm and a length of 50 mm was prepared. The pin was ready as a non-threaded type with lengths of 1, 2, and 3.5 mm, depending on the selected aluminum sheet thickness, while the diameter was maintained as a constant (3 mm). The welding tool was made from carbon steel with a carbon content of up to 1.5%. It was characterized by high hardness, wear resistance, and thermal stability, making it efficient at generating heat through friction.

Figure 2 shows the lap joint configuration of the aluminum alloy specimens. A load cell was used to measure the normal force exerted by the welding tool on the specimen surface, with the signal converted to digital using an analog-to-digital converter (U3-LV, LabJack, USA). A welding platform was also prepared to securely hold the specimens. A thermal imaging camera (TC002, TOPDON, USA), compatible with smartphones, was used to monitor temperature evolution during and after welding by tracking temperature loss and decline over time. The thermal camera has a resolution of 256 × 192 pixels and a high heat sensitivity of 40 mK. The chemical composition of the AA 6061 alloys, as measured using a metal analyzer (SPECTROPORT PXC01, AMETEK, USA), is presented in Table 2. Table 2 also shows the mechanical properties of AA 6061 aluminum.

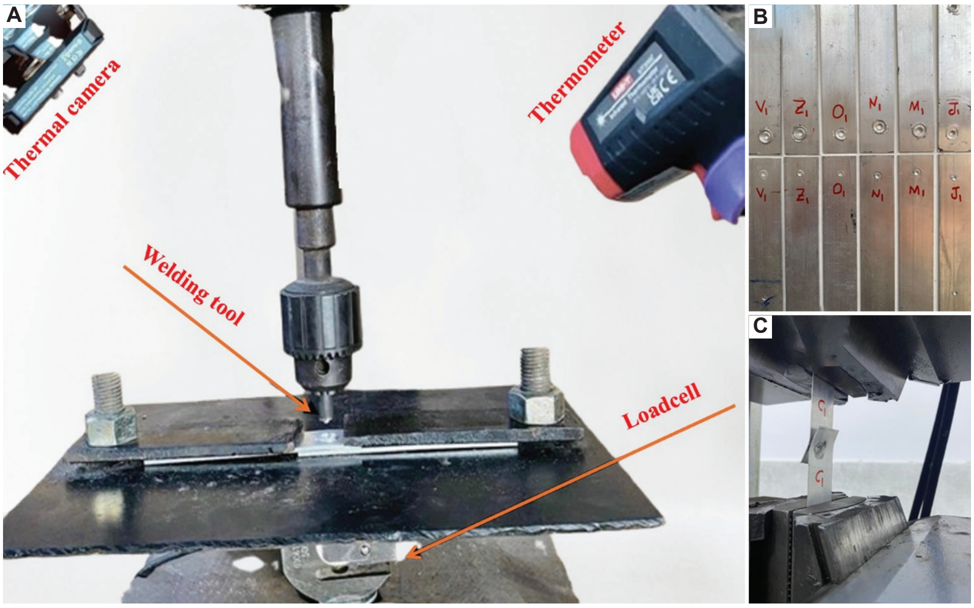

Figure 2. Friction stir spot welding process. (A) Welding arrangements; (B) Welded specimens; (C) Lap-shear tensile test.

Table 2. Characteristics of AA 6061 aluminum

Characteristics	Value
Chemical composition (element, %)	
Chromium	0.260
Copper	0.340
Magnesium	1.080
Iron	0.660
Silicon	0.550
Manganese	0.110
Titanium	0.160
Zinc	0.223
Aluminum	96.617
Mechanical properties	
Hardness (HV)	40
Yield strength (MPa)	276
Tensile strength (MPa)	310

Due to the nonlinearity in predicting the maximum thermal and tensile responses of the FSSW joint, this topic remains actively studied. This study was designed to predict the maximum temperature (°C) and the maximum lap-shear fracture load (kN) from FSSW process parameters. The total number of specimens used in this study was 81; every three specimens were examined with the same input parameters. The parameters involved were sheet thickness (mm), tool rotational speed (rpm), and dwelling time (s). The selected input parameter values were based on previous studies. The average of each of the three specimens was calculated. Table 3 shows the values of the welding parameters used, the corresponding maximum temperatures, and lap-shear fracture loads. The EDA and ML techniques were then used to maximize output response for temperature and lap-shear fracture load.

3. Results and discussion

3.1. Evaluation of EDA

This study employed EDA to analyze sets of experimental results obtained during the FSSW process. Several specific procedures were followed to ensure the accuracy of the results. The input parameters were aluminum sheet thickness, dwelling time, and tool rotational speed. The primary purpose of using EDA is to provide a deep, comprehensive understanding of the dataset characteristics and their relationship with the output variables—maximum temperature (°C) and lap-shear fracture load (kN). Histograms were plotted to visualize the distribution of key input parameters: thickness (mm) (Figure 3), rotational speed (rpm) (Figure 4), and dwell time (s) (Figure 5). These visualizations revealed variations in parameter distributions, highlighting potential areas of skewness or concentration.

Binning is a practical preprocessing method that simplifies complex data during exploratory analysis. By grouping raw continuous values into manageable intervals—or “bins”—this technique reduces noise and identifies underlying trends.[55] For the x-axis in Figures 3-5, binning was used to group the 27 original datasets into eight intervals, yielding clean, representative bar graphs that highlighted meaningful patterns.

Table 3. Friction stir spot welding process parameters and corresponding output parameters

No.	Thickness (mm)	Rotation speed (rpm)	Dwelling time (s)	Max temperature (°C)	Lap-shear fracture load (kN)
1	1	1,000	3	74	1.23
2	1	1,500	3	102	1.42
3	1	2,000	3	112	1.61
4	1	1,000	6	93	1.33
5	1	1,500	6	139	1.52
6	1	2,000	6	166	1.73
7	1	1,000	9	125	1.55
8	1	1,500	9	147	2.00
9	1	2,000	9	176	2.20
10	2	1,000	3	85	1.20
11	2	1,500	3	115	1.34
12	2	2,000	3	128	1.53
13	2	1,000	6	96	1.65
14	2	1,500	6	133	1.84
15	2	2,000	6	165	2.19
16	2	1,000	9	132	2.26
17	2	1,500	9	153	2.33
18	2	2,000	9	179	2.59
19	3	1,000	3	97	1.51
20	3	1,500	3	126	1.82
21	3	2,000	3	138	2.11
22	3	1,000	6	118	1.84
23	3	1,500	6	148	2.14
24	3	2,000	6	187	2.35
25	3	1,000	9	136	2.13
26	3	1,500	9	180	2.36
27	3	2,000	9	215	2.54

Figure 3 presents the histogram for aluminum sheet thickness during the FSSW process. The statistics reveal a standard deviation of approximately 0.832 over the 1–3 mm range, with a median value of 2 mm. The 25th, 50th, and 75th percentiles are 1, 2, and 3 mm, respectively, indicating a reasonably symmetric distribution around the median. Such a balanced distribution is critical, as it indicates the dataset is free from significant skewness or extreme outliers that could otherwise distort the analysis.[55]

The histogram of aluminum sheet thickness did not differ significantly from that of tool rotation speed (Figure 4) and dwelling time (Figure 5), with a symmetric distribution centered around the mean. The standard deviations were 392.558 and 2.496 for the tool rotational speed and the dwelling time, respectively. The 25th, 50th, and 75th percentiles of the rotational speeds were 1,000 rpm, 1,500 rpm, and 2,000 rpm, respectively, while those of the dwelling times were 3 s, 6 s, and 9 s, respectively.

EDA, a crucial component of the FSSW process analysis in this study, involved generating correlations between thermal behavior and mechanical behavior maps to visualize linear relationships between pairs of variables during the FSSW of the aluminum alloy.

A correlation heat map is typically used to display the strength and direction of linear relationships between numerical variables in a dataset. The correlation values ranged from −1 to +1, while 0 indicates no linear correlation, −1 indicates a strong negative correlation (as one variable increases, the other decreases), and +1 indicates a strong positive correlation (both variables increase together). Moreover, the heat map shows a color-coded matrix, in which darker colors indicate stronger correlations, while lighter or neutral colors indicate weaker or no correlation.

In FSSW studies, the correlation heat map reveals how welding parameters, such as thickness, rotational speed, and dwell time, correlate with output responses, including maximum temperature and lap-shear fracture load. Figure 6 shows the heat map of correlations among the variables in this study. A value of 1.00 indicates perfect correlation, whereas values close to 0 indicate weak or no correlation. There are strong links between maximum temperature and lap-shear fracture load (r = 0.86) and between dwelling time and lap-shear fracture load (r = 0.96). At the same time, there is a weak correlation between thickness and maximum temperature (r = 0.28).

It is crucial to verify the significance of features in ML algorithms after model training, as it measures the impact of each variable (feature) on the model's results, reveals the contribution of each input to the output values, and identifies the most influential variables. This study used feature significance as a linear regression model to illustrate the impact of friction welding process parameters (dwell time, sheet thickness, and tool rotation speed) on the process outputs (maximum temperature and lap-shear fracture load).

Dwell time demonstrated the highest feature importance for lap-shear strength, indicating it most strongly influences weld quality. The feature importance of dwelling time was 0.28, corresponding to lower values for sheet thickness (0.19) and tool rotational speed (0.18), as shown in Figure 7. The most significant impact of dwell time, as the highest feature importance for lap-shear strength, might be attributed to greater frictional heating between the tool and the workpieces. The increase in

 doi: 10.36922/IJAMD025360032

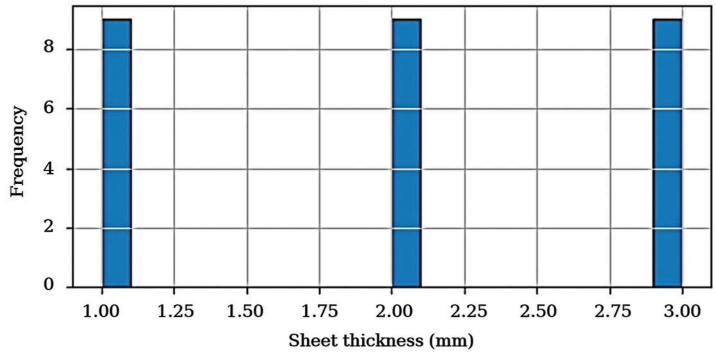

Count	27.000
Mean	2.0000
Std	0.8320
Min	1.0000
25th percentile	1.0000
50th percentile	2.0000
75th percentile	3.0000
Max	3.0000

Figure 3. Histogram analysis of the aluminum sheet thickness (mm) during the friction stir spot welding

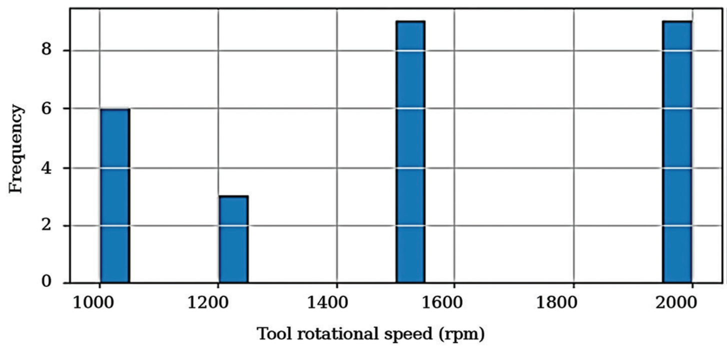

Count	27.0000
Mean	1522.22
Std	392.558
Min	1000.00
25th percentile	1200.00
50th percentile	1500.00
75th percentile	2000.00
Max	2000.00

Figure 4. Histogram analysis of the tool rotational speed (rpm) during the friction stir spot welding

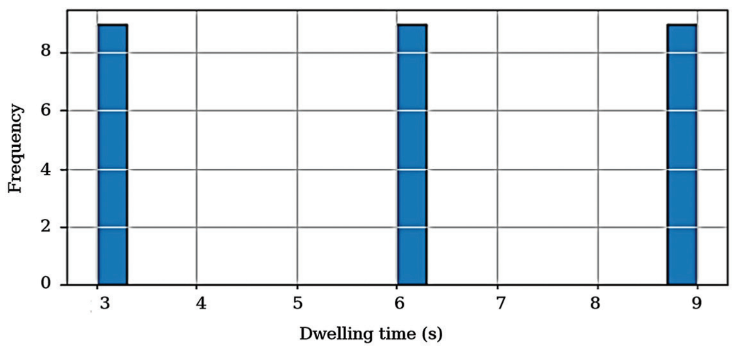

Count	27.000
Mean	6.0000
Std	2.4961
Min	3.0000
25th percentile	3.0000
50th percentile	6.0000
75th percentile	9.0000
Max	9.0000

Figure 5. Histogram analysis of the dwelling time (s) during the friction stir spot welding

dwelling time extended the time the tool spent rotating in the weld pool, resulting in greater homogeneity and mixing between the two aluminum plates during the FSSW process. This improved mixing and homogeneity ultimately led to increased shear forces and enhanced mechanical properties.

Figure 7 reflects the nature of the specimens in FSSW. The lower the dwell time, the poorer the joint quality, and thereby the weaker the tensile strength. Conversely, a longer dwell time resulted in a rigid joint, requiring a greater force to cause failure and lap fracture, as shown in Table 4 (tool rotational speed of 1,500 rpm and aluminum sheet thickness of 3 mm).

Tool rotational speed had the largest influence on maximum temperature, with a feature importance of 22.72. However, dwell time did not significantly affect the maximum temperature, with a feature importance of 21.13, slightly lower than that of tool rotation speed. The effect of aluminum sheet thickness was small, accounting for approximately 48% of the total effect, compared to the effects of rotation speed and dwell time, with a feature importance of 9.57, as shown in Figure 8.

The thermal imaging temperature readings confirm the EDA results. Under constant-sheet-thickness aluminum samples (2 mm) and a constant dwelling time (6 s), the controlled increase in rotational speed from 1,000 to

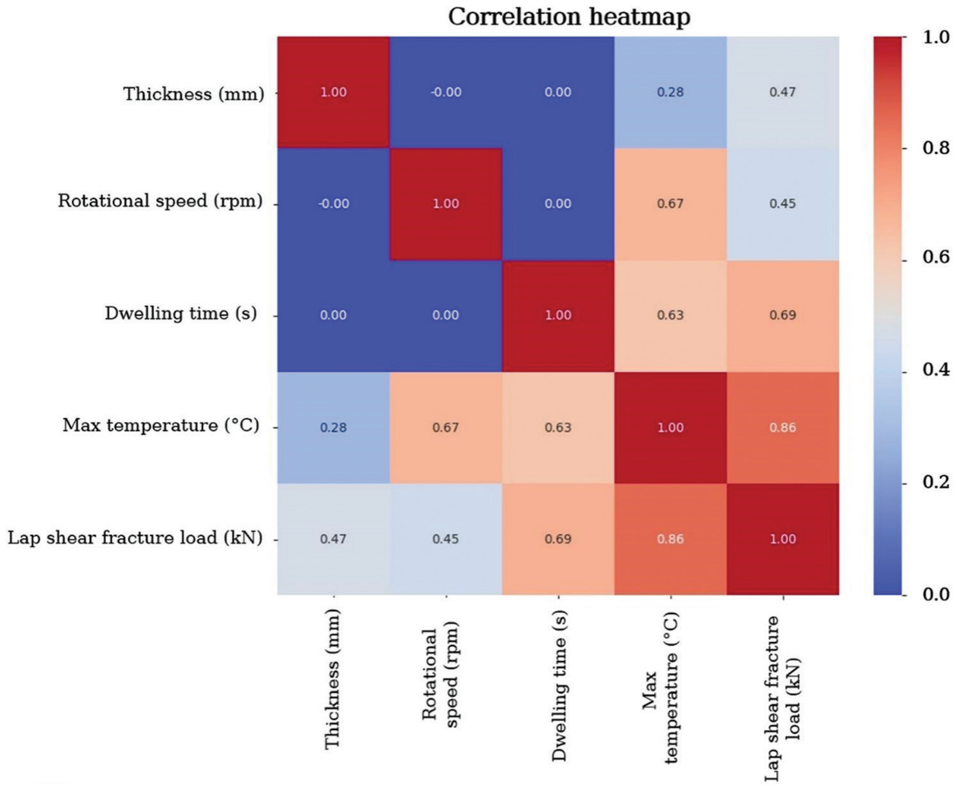

Figure 6. Correlation heatmap for the input and output parameters during the friction stir spot welding

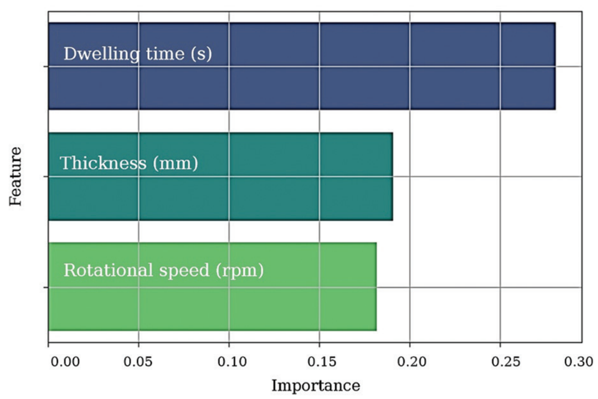

Figure 7. Feature importance analysis of the friction stir spot welding process parameters on the lap-shear fracture load

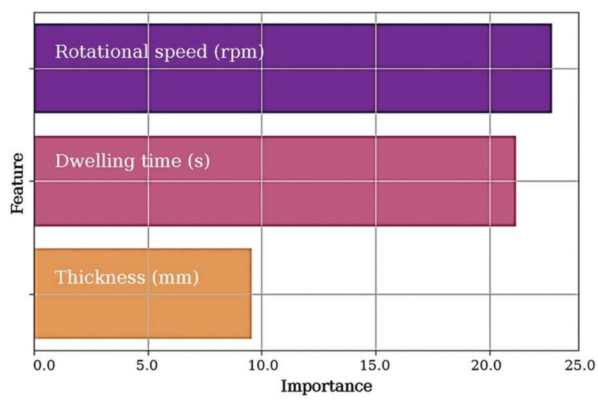

Figure 8. Feature importance analysis of the friction stir spot welding process parameters on maximum temperature

2,000 rpm, with a 500 rpm step, led to nonlinear behavior in the generated temperature of 96°C, 133°C, and 165°C, respectively, as shown in Figure 9. The increase in temperature can be attributed to increased frictional heat generation and the intensification of plastic deformation as the rotational speed increases.

3.2. Effectiveness of ML predictions

This study examined and compared several ML algorithms. Random forest, elastic net, Bayesian ridge, polynomial regression, and robust regression were used to predict thermal behavior (maximum temperature) and the mechanical behavior (lap-shear fracture load) during the FSSW process. Mean squared error (MSE), mean absolute error (MAE), and coefficient of determination (R^2) were used to evaluate the ML models. MSE measures the average squared prediction error; lower values indicate that the predictions are closer to the actual values. Moreover, it penalizes larger errors heavily, making it useful when large deviations in the FSSW process are undesirable. MAE is

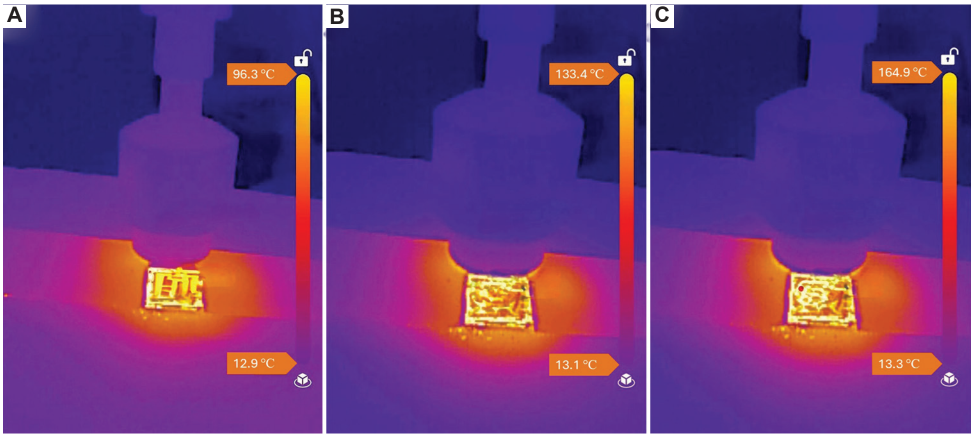

Figure 9. Effect of rotational speed on the maximum temperature in the friction stir spot welding process at a dwelling time of 6 sec and a sheet thickness of 2 mm. (A) 1,000 rpm; (B) 1,500 rpm; (C) 2,000 rpm.

Table 4. Effect of dwelling time of lap-shear fracture in friction stir spot welding at 1,500 rpm and 3 mm thickness

Dwelling time (s)	Lap-shear fracture load (kN)	Joint after FSSW	Joint after fracture
3	1.82		
6	2.14		
9	2.36	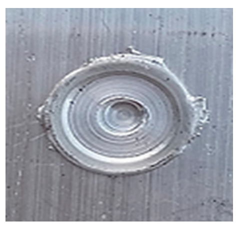	

Abbreviations: FSSW: Friction stir spot welding.

the average of the absolute differences between predictions and actual values during the FSSW process; lower MAE values indicate higher average prediction accuracy. The coefficient of determination (R^2) is an indicator of how well the independent variables explain the variance in the dependent variable during the experimental process. Their values ranged from 0 to 1, depending on the model that provided the better fit. The following subsections will examine the accuracy of the ML algorithms based on the obtained values of MSE, MAE, and R^2.

3.2.1. Evaluation of ML models in predicting thermal behavior

The total number of FSSW parameter sets examined in this section is 27. All selected ML models (random forest algorithm, elastic net regression, Bayesian ridge regression, SVR, polynomial regression, and robust regression) were evaluated using MSE, MAE, and R^2. This step is essential for both linear and nonlinear regression algorithms to compare the efficacy of ML models. Figure 10 shows significantly lower MSE values for all ML models, except SVR, indicating suitable performance across all algorithms. The high MSE in SVR compared to other models suggests poor performance in predicting maximum temperatures. This ineffective behavior of the SVR may be due to the applied SVR kernel struggling to capture complex, nonlinear relationships between input features (like thickness, speed, and dwell time) and the corresponding temperature. Moreover, in numerous engineering applications, SVR can be data-sensitive, leading to poor generalization and higher errors.[56]

The random forest algorithm demonstrated superior performance (MSE = 26.51) in predicting maximum temperature due to its ability to model complex relationships, such as those in the FSSW process, between FSSW process parameters and output responses. Moreover, random forest is robust to outliers and noise, which are often present in experimental welding datasets.

Figure 11 shows the MAE values of various ML methods applied to temperature prediction during the FSSW process. A notable observation is the strong alignment between the MSE and MAE results. Although these two metrics differ in how they mathematically penalize errors and handle outliers, their parallel behavior here confirms that they provide a consistent assessment of the models' prediction accuracy. Notably, the experimental data were collected under the supervision of highly experienced FSSW personnel, resulting in very few, if any, outliers. This approach led to greater prediction stability for all ML approaches used in this study.

Figure 12 displays the R^2 values of various regression models. Models such as the random forest algorithm, elastic net regression, Bayesian ridge regression, polynomial regression, and robust regression algorithm achieved high R^2 values, indicating that they explained a large portion of the variance in the data and thus demonstrated better predictive power. In contrast, the SVR exhibited low R^2 values, suggesting poor performance in explaining the data's variance. The comparative analysis of the models using MSE, MAE, and R^2 scores highlights several key findings. The random forest algorithm model stands out with the lowest MSE (26.51) and MAE (3.86), along with the highest R^2 score (0.97), demonstrating exceptional prediction accuracy and a strong fit to the data.

The polynomial regression model also exhibited robust performance with low MSE (51.63) and MAE (6.26), and a high R^2 score (0.95). Similarly, Bayesian ridge regression

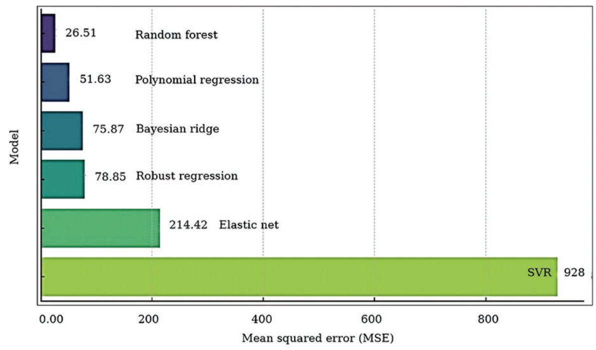

Figure 10. Evaluation of machine learning algorithms in maximum temperature prediction using mean squared error during the friction stir spot welding process
Abbreviation: SVR: Support vector regression.

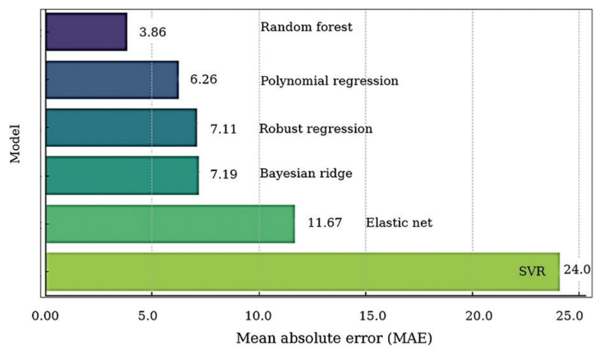

Figure 11. Evaluation of machine learning algorithms in maximum temperature prediction using mean absolute error during the friction stir spot welding process
Abbreviation: SVR: Support vector regression.

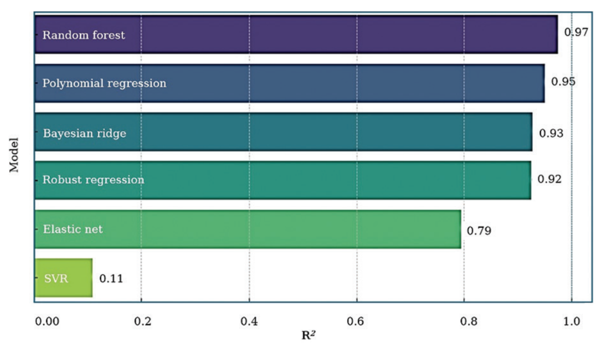

Figure 12. Evaluation of machine learning algorithms in maximum temperature prediction using R^2 during the friction stir spot welding process
Abbreviation: SVR: Support vector regression.

demonstrated remarkably low MSE (75.87), low MAE (7.19), and a high R^2 score (0.93), indicating its effectiveness.

On the other hand, with high MSE (928.44), MAE (24.09), and a low R^2 score (0.11), SVR performs poorly, indicating that it is the least appropriate model without additional adjustment. Except for the elastic net, which yielded an R^2 of 0.7, other models exhibited strong R^2 values, making them suitable for temperature prediction. For applications requiring high predictive precision, the random forest, robust regression, polynomial regression, and Bayesian ridge regression models are recommended.

This study reports poor/good SVR responses in thermal and tensile performance, respectively. Temperature is monitored in real time using an infrared thermometer and thermal camera throughout the welding process. Due to the high nonlinearity of the friction temperature at the interface between the pin and the shoulder bottom, which are in contact with the aluminum alloy specimens, it is difficult to control the temperature and to tune the model or use SVR kernels to capture it effectively. The poor performance of SVR relative to other ML models in thermal applications, such as welding, has been well documented in previous studies.[57] Careful specimen preparation and controlled testing conditions likely reduced experimental variability, which may have improved model performance for tensile outcomes. The mechanical properties exhibited consistent, stable relationships with the input features, making them amenable to SVR modeling with the chosen parameters. Therefore, the SVR performed better in predicting mechanical properties than thermal behavior. This better SVR performance related to other ML techniques was also noticed in previous studies.[39]

3.2.2. Evaluation of ML models in predicting mechanical behavior

The total number of FSSW parameter sets examined in this section is 27. The previously mentioned models were also used to study and predict the mechanical properties of the weld joint and to compare them based on MSE, MAE, and R^2. The elastic net model yielded an MSE of 0.16, indicating poor model performance in this process. In contrast, the random forest, SVR, Bayesian ridge, and polynomial regression models exhibited favorable performance, with MSE values below 0.02, as shown in Figure 13. In contrast, Figure 14 compares the ML algorithms based on the MAE for predicting the maximum lap-shear fracture load. The lowest MAE values were observed with the random forest, SVR, and robust regression algorithms, at 0.07, 0.08, and 0.09, respectively. On the other hand, the elastic net model yielded a high value of 0.3, indicating poor performance in predicting the tensile performance of the FSSW weld joint, as indicated by the MAE.

Figure 15 displays the R^2 values as a bar chart of various regression models for the prediction of maximum lap-shear fracture load. Models such as the random forest

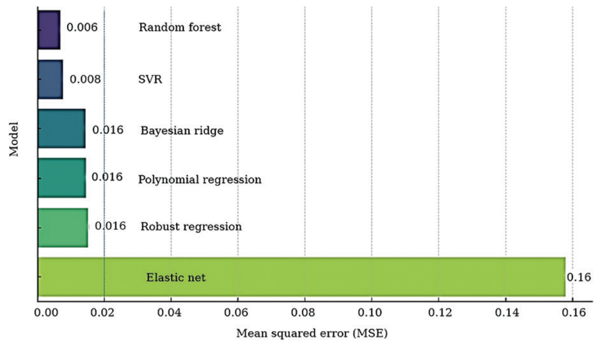

Figure 13. Evaluation of machine learning algorithms in predicting maximum lap-shear fracture load of weld joint using mean squared error during the friction stir spot welding process
Abbreviation: SVR: Support vector regression.

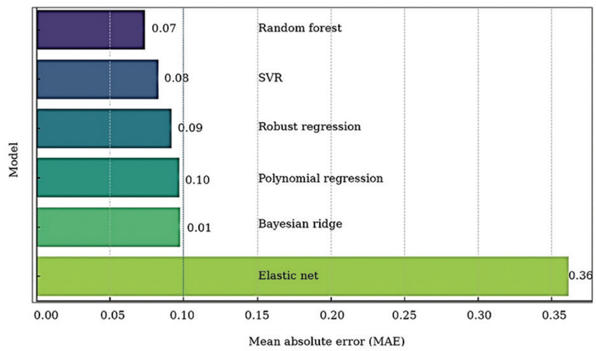

Figure 14. Evaluation of machine learning algorithms in predicting the maximum lap-shear fracture load of the weld joint using the mean absolute value during the friction stir spot welding process
Abbreviation: SVR: Support vector regression.

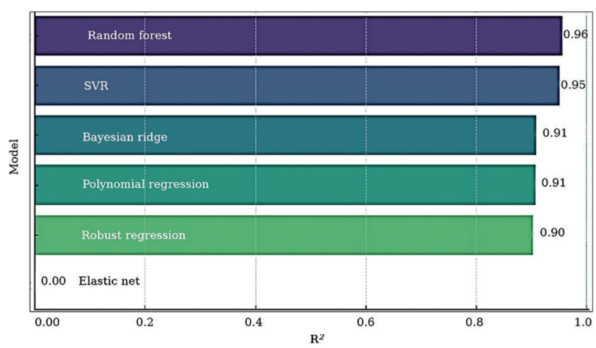

Figure 15. Evaluation of machine learning algorithms in predicting the maximum lap-shear fracture load of the weld joint using the coefficient of determination (R^2) during the friction stir spot welding process
Abbreviation: SVR: Support vector regression.

algorithm, elastic net regression, Bayesian ridge regression, polynomial regression, and robust regression algorithm achieve high R^2 values. All models recorded excellent performance in predicting the mechanical properties of the weld joint with R^2 values approaching 0.9, except for the elastic net regression model, which showed inaccuracy and poor performance of $R^2 = 0$.

Based on the evaluation and comparison of models, R^2, MAE, and MSE, the elastic net regression model showed the weakest performance in terms of predicting the mechanical performance of the weld joint, as it recorded the lowest value for $R^2 = 0$, MAE = 0.36, and MSE = 0.16.

4. Conclusion

The major research question in this study concerns the feasibility of using EDA and ML approaches to determine the optimal thermal and tensile performances of aluminum joints welded using FSSW. The main challenge focuses on modeling the nonlinear behavior of the FSSW process outputs. The key findings that can be concluded from this study are as follows:

(i) In the FSSW process, there is no single model that can be relied upon for evaluation and prediction to suit all objectives, as the outcome depends on the variables of the welding process. In general, high-flexibility algorithms, such as the random forest algorithm and polynomial regression, have proven effective for predicting welding process outputs because they handle nonlinear relationships. The SVR model did not yield satisfactory results in determining the optimal thermal or mechanical performance of FSSW within the specified welding parameters. In contrast, Bayesian ridge regression, while not performing as well as the random forest algorithm, is considered satisfactory and can be recommended.

(ii) ML models are suitable tools to determine input variables. The dwelling time may have the highest significance (0.28) for the lap-shear fracture load, indicating that it significantly affects weld quality. In contrast, the tool rotation speed had the greatest impact on the maximum temperature, with a feature importance of 22.72.

(iii) The evaluation of ML models using MSE, MAE, and R^2 is essential for comparing the ML algorithms that can be used to predict thermal and tensile performance of the FSSW process.

The application of EDA—limited in this study to determining relationships among welding process variables for algorithm selection—together with ML techniques provided valuable insights into the thermal and mechanical behavior of the resulting joints. These results suggest that the proposed approach may serve as an effective analytical framework for complex solid-state welding processes, including repetitive friction-flip welding and double friction-flip welding. For future studies, ML techniques may be combined with X-ray diffraction images to classify joint defects and to accurately investigate metallic effects in friction-flip weld joints.

Acknowledgments

None.

Funding

None.

Conflict of interest

The authors declare that they have no competing interests.

Author contributions

Conceptualization: Raheem Al-Sabur
Formal analysis: Sajad N. Alasadi
Investigation: All authors
Methodology: Sajad N. Alasadi
Writing–original draft: Sajad N. Alasadi
Writing–review & editing: Raheem Al-Sabur

Ethics approval and consent to participate

Not applicable.

Consent for publication

Not applicable.

Availability of data

The data presented in this study are available upon request from the corresponding author.

References

1. Chen H, Zhu Z, Zhu Y, Sun L, Guo Y. Solid-state welding of aluminum to magnesium alloys: A review. *Metals (Basel)*. 2023;13(8):1410.

   doi: 10.3390/met13081410

2. Khedr M, Hamada A, Järvenpää A, Elkatatny S, Abd-Elaziem W. Review on the solid-state welding of steels: Diffusion bonding and friction stir welding processes. *Metals (Basel)*. 2023;13(1):54.

   doi: 10.3390/met13010054

3. Badavath HJ, Chattopadhyay S, Shankar S. Solid-State Welding and its Applications: A Methodological Review. In: *AIP Conference Proceedings*. Vol. 2681; 2022.

   doi: 10.1063/5.0116893

4. Gibson BT, Lammlein DH, Prater TJ, *et al*. Friction stir welding: Process, automation, and control. *J Manuf Process*. 2014;16(1):56-73.

   doi: 10.1016/j.jmapro.2013.04.002

5. Majeed T, Wahid MA, Alam MN, Mehta Y, Siddiquee AN. Friction stir welding: A sustainable manufacturing process. In: *Materials Today: Proceedings*. Vol. 46; 2020.

doi: 10.1016/j.matpr.2021.04.025

6. Khalaf HI, Al-Sabur R. Friction stir techniques exploring fracture and fatigue behavior in hybrid composite joints. In: *Utilizing Friction Stir Techniques for Composite Hybridization*. United States: IGI Global; 2024. p. 108-134.

doi: 10.4018/979-8-3693-3993-0.ch007

7. Avettand-Fènoël MN, Simar A. A review about friction stir welding of metal matrix composites. *Mater Charact*. 2016;120:1-17.

doi: 10.1016/j.matchar.2016.07.010

8. Belalia SE, Serier M, Al-Sabur R. Parametric analysis for torque prediction in friction stir welding using machine learning and shapley additive explanations. *J Computat Appl Mech*. 2024;55(1):113-124.

doi: 10.22059/JCAMECH.2024.370055.924

9. Tiwari A, Singh P, Pankaj P, Biswas P, Kore SD. FSW of low carbon steel using tungsten carbide (WC-10wt.%Co) based tool material. *J Mech Sci Technol*. 2019;33(10):4931-4938.

doi: 10.1007/s12206-019-0932-7

10. Serier M, Jassim RJ, Al-Sabur R, Siddiquee AN. Thermal Diffusivity Modeling for Aluminum AA6060 Plates During Friction Stir Welding. In: *AIP Conference Proceedings*. Vol. 3051; 2024.

doi: 10.1063/5.0191742

11. Jassim AK, Al-Subar RK. Studying the possibility to Weld AA1100 aluminum alloy by friction stir spot welding. *Int J Mater Metall Eng*. 2017;11(9):660.

12. Borah MJ, Saha N. Effect of Tool Geometry and Process Parameters on Strength of Various Friction Stir Spot Welded Lap Joints. In: *Proceedings of the World Congress on Mechanical, Chemical, and Material Engineering*; 2019.

doi: 10.11159/icmie19.124

13. Al-Sabur R, Serier M. Material sustainability during friction stir joining. In: *Sustainable Machining and Green Manufacturing*. United States: Wiley; 2024.

doi: 10.1002/9781394197866.ch7

14. Sree Sabari S, Malarvizhi S, Balasubramanian V. Characteristics of FSW and UWFSW joints of AA2519-T87 aluminium alloy: Effect of tool rotation speed. *J Manuf Process*. 2016;22:278-289.

doi: 10.1016/j.jmapro.2016.03.014

15. Alasdi SN, Al-Sabur R. In-depth thermal analysis of different pin configurations in friction stir spot welding of similar and dissimilar alloys. *J Manuf Mater Process*. 2025;9(6):184.

doi: 10.3390/jmmp9060184

16. Marazani T, Jeje SO, Shongwe MB, Malatji N. Mass flash reduction strategies in friction stir processing of aluminum alloys: A review. *Eng Rep*. 2024;6(10):e12981.

doi: 10.1002/eng2.12981

17. Morgenthaler S. Exploratory data analysis. *Wiley Interdiscip Rev Comput Stat*. 2009;1(1):33-44.

doi: 10.1002/wics.2

18. Bezerra A, Silva I, Guedes LA, Silva D, Leitão G, Saito K. Extracting value from industrial alarms and events: A data-driven approach based on exploratory data analysis. *Sensors (Basel)*. 2019;19(12):2772.

doi: 10.3390/s19122772

19. Mathew BK, Velmurugan C, Vanitha V. Estimating Most Influencing Parameter in TIG Welding of SS304 Using Exploratory Data Analysis. In: *2021 International Conference on Advancements in Electrical, Electronics, Communication, Computing and Automation, ICAECA 2021*; 2021.

doi: 10.1109/ICAECA52838.2021.9675521

20. Wang LC. Experience of data analytics in EDA and test - Principles, promises, and challenges. *IEEE Trans Comput Aided Des Integr Circ Syst*. 2017;36(6):885-898.

doi: 10.1109/TCAD.2016.2621883

21. Alzubi J, Nayyar A, Kumar A. Machine learning from theory to algorithms: An overview. *J Phys Conf Ser*. 2018;1142:012012.

doi: 10.1088/1742-6596/1142/1/012012

22. Tufail S, Riggs H, Tariq M, Sarwat AI. Advancements and challenges in machine learning: A comprehensive review of models, libraries, applications, and algorithms. *Electronics (Switzerland)*. 2023;12(8):1789.

doi: 10.3390/electronics12081789

23. Wang Z, Li L, Chen H, *et al.* Penetration recognition based on machine learning in arc welding: A review. *Int J Adv Manuf Technol*. 2023;125(9-10):3899-3923.

doi: 10.1007/s00170-023-11035-7

24. Maculotti G, Genta G, Galetto M. Optimisation of laser welding of deep drawing steel for automotive applications by Machine Learning: A comparison of different techniques. *Qual Reliab Eng Int*. 2024;40(1):202-219.

doi: 10.1002/qre.3377

25. Sun H, Ramuhalli P, Jacob RE. Machine learning for ultrasonic nondestructive examination of welding defects: A systematic review. *Ultrasonics*. 2023;127:106854.

doi: 10.1016/j.ultras.2022.106854

26. Zhou B, Pychynski T, Reischl M, Kharlamov E, Mikut R. Machine learning with domain knowledge for predictive quality monitoring in resistance spot welding. *J Intell Manuf*. 2022;33(4):1139-1163.

doi: 10.1007/s10845-021-01892-y

27. Yu F, Zhao Y, Lin Z, Miao Y, Zhao F, Xie Y. Prediction of mechanical properties and optimization of friction stir welded 2195 aluminum alloy based on BP neural network. *Metals (Basel)*. 2023;13(2):267.

    doi: 10.3390/met13020267

28. Verma S, Msomi V, Mabuwa S, *et al*. Machine learning application for evaluating the friction stir processing behavior of dissimilar aluminium alloys joint. *Proc Instit Mech Eng L J Mater Des Appl*. 2022;236(3):633-646.

    doi: 10.1177/14644207211053123

29. Elsheikh AH. Applications of machine learning in friction stir welding: Prediction of joint properties, real-time control and tool failure diagnosis. *Eng Appl Artif Intell*. 2023;121:105961.

    doi: 10.1016/j.engappai.2023.105961

30. Chadha U, Selvaraj SK, Gunreddy N, *et al*. A Survey of machine learning in friction stir welding, including unresolved issues and future research directions. *Mater Des Process Commun*. 2022;2022:2568347.

    doi: 10.1155/2022/2568347

31. Ebnonnasir A, Karimzadeh F, Enayati MH. Novel artificial neural network model for evaluating hardness of stir zone of submerge friction stir processed Al 6061-T6 plate. *Mater Sci Technol*. 2011;27(6):990-995.

    doi: 10.1179/174328409X425290

32. Dinaharan I, Palanivel R, Murugan N, Laubscher RF. Application of artificial neural network in predicting the wear rate of copper surface composites produced using friction stir processing. *Aust J Mech Eng*. 2022;20(4):1079-1090.

    doi: 10.1080/14484846.2020.1769803

33. Pattanaik AK, Pal K, Mishra D. Tribiological investigation and optimization of friction stir spot welding of dissimilar metals by LSSM-ANN method. *Mech Based Des Struct Mach*. 2022;50(5):1595-1613.

    doi: 10.1080/15397734.2020.1759429

34. Manvatkar VD, Arora A, De A, DebRoy T. Neural network models of peak temperature, torque, traverse force, bending stress and maximum shear stress during friction stir welding. *Sci Technol Weld Join*. 2012;17(6):460-466.

    doi: 10.1179/1362171812Y.0000000035

35. Matitopanum S, Pitakaso R, Sethanan K, Srichok T, Chokanat P. Prediction of the ultimate tensile strength (UTS) of asymmetric friction stir welding using ensemble machine learning methods. *Processes*. 2023;11(2):460-466.

    doi: 10.3390/pr11020391

36. Bhat NN, Kumari K, Dutta S, Pal SK, Pal S. Friction stir weld classification by applying wavelet analysis and support vector machine on weld surface images. *J Manuf Process*. 2015;20:274-281.

    doi: 10.1016/j.jmapro.2015.07.002

37. Sefene EM, Tsegaw AA, Mishra A. Process parameter optimization of 6061AA friction stir welded joints using supervised machine learning regression-based algorithms. *J Soft Comput Civil Eng*. 2022;6(1):274-281.

    doi: 10.22115/SCCE.2022.299913.1350

38. Bock FE, Paulsen T, Brkovic N, *et al*. Evaluation of Mechanical Property Predictions of refill Friction Stir Spot Welding Joints via Machine Learning Regression Analyses on DoE Data. In: *ESAFORM 2021 - 24th International Conference on Material Forming*; 2021.

    doi: 10.25518/esaform21.2589

39. Mothilal M, Kumar A. Predictive modeling of ultimate tensile strength in dissimilar friction stir welded aluminum alloys via machine learning approach. *Philos Mag Lett*. 2025;105(1):2472669.

    doi: 10.1080/09500839.2025.2472669

40. Sambath Y, Natarajan R, Babu PK, *et al*. Comparative analysis of predictive modeling techniques for mechanical properties in dissimilar friction stir welding of AA6061 and AZ31B. *J Mater Eng Perform*. 2025;34:15597-15613.

    doi: 10.1007/s11665-024-10317-9

41. El-Said EMS, Abd Elaziz M, Elsheikh AH. Machine learning algorithms for improving the prediction of air injection effect on the thermohydraulic performance of shell and tube heat exchanger. *Appl Therm Eng*. 2021;185:116471.

    doi: 10.1016/j.applthermaleng.2020.116471

42. Ramesh K, Ramana EV, Srikanth L, Sri Harsha C, Kiran Kumar N. Identification of SMAW surface weld defects using machine learning. In: *Lecture Notes in Mechanical Engineering*. Berlin: Springer; 2023.

    doi: 10.1007/978-981-19-5347-7_28

43. Tsai YA, Lo YL, Raza MM, *et al*. Optimization of lap-joint laser welding parameters using high-fidelity simulations and machine learning mode. *J Mater Res Technol*. 2023;24:6876-6892.

    doi: 10.1016/j.jmrt.2023.04.256

44. España VJ, Aparicio J, Barber X. An adaptation of Random Forest to estimate convex non-parametric production technologies: An empirical illustration of efficiency measurement in education. *Int Trans Oper Res*. 2025;32(5):2523-2546.

    doi: 10.1111/itor.13561

45. Tabib S, Larocque D. Non-parametric individual treatment effect estimation for survival data with random forests. *Bioinformatics*. 2020;36(2):629-636.

    doi: 10.1093/bioinformatics/btz602

46. Zhang Z, Yang Z, Ren W, Wen G. Random forest-based real-time defect detection of Al alloy in robotic arc welding using optical spectrum. *J Manuf Process*. 2019;42:51-59.

doi: 10.1016/j.jmapro.2019.04.023

47. Zhu C, Yuan H, Ma G. An active visual monitoring method for GMAW weld surface defects based on random forest model. *Mater Res Express*. 2022;9(3):036503.

doi: 10.1088/2053-1591/ac5a38

48. Strobl C, Malley J, Tutz G. An introduction to recursive partitioning: Rationale, application, and characteristics of classification and regression trees, bagging, and random forests. *Psychol Methods*. 2009;14(4):323-348.

doi: 10.1037/a0016973

49. Zhang Z, Lai Z, Xu Y, Shao L, Wu J, Xie GS. Discriminative elastic-net regularized linear regression. *IEEE Trans Image Process*. 2017;26(3):1466-1481.

doi: 10.1109/TIP.2017.2651396

50. Martín Ó, Ahedo V, Santos JI, De Tiedra P, Galán JM. Quality assessment of resistance spot welding joints of AISI 304 stainless steel based on elastic nets. *Mater Sci Eng A*. 2016;676:173-181.

doi: 10.1016/j.msea.2016.08.112

51. Michimae H, Emura T. Bayesian ridge estimators based on copula-based joint prior distributions for regression coefficients. *Comput Stat*. 2022;37(5):2741-2769.

doi: 10.1007/s00180-022-01213-8

52. Šket K, Brezočnik M, Karner T, *et al.* Predictive modelling of weld bead geometry in wire arc additive manufacturing. *J Manuf Mater Process*. 2025;9(2):67.

doi: 10.3390/jmmp9020067

53. Hinkle J, Muralidharan P, Fletcher PT, Joshi S. Polynomial regression on Riemannian manifolds. In: *Lecture Notes in Computer Science (Including Subseries Lecture Notes in Artificial Intelligence and Lecture Notes in Bioinformatics)*. Vol 7574. Berlin: Springer; 2012.

doi: 10.1007/978-3-642-33712-3_1

54. Liu C, Li B, Vorobeychik Y, Oprea A. Robust linear regression against training data poisoning. In: *AISec 2017 - Proceedings of the 10th ACM Workshop on Artificial Intelligence and Security, Co-Located with CCS 2017*; 2017.

doi: 10.1145/3128572.3140447

55. Sandfeld S. Exploratory Data Analysis. In: *Materials Data Science. The Materials Research Society Series*. Cham: Springer; 2024. p. 179-206.

doi: 10.1007/978-3-031-46565-9_9

56. Li S, Li M, Liu Z, Li M. A Data-Driven Residual Life Prediction Method for Rolling Bearings. In: *Proceedings of 2023 IEEE 12th Data Driven Control and Learning Systems Conference, DDCLS 2023*; 2023.

doi: 10.1109/DDCLS58216.2023.10166951

57. Anandan B, Manikandan M. Machine learning approach for predicting the peak temperature of dissimilar AA7050-AA2014A friction stir welding butt joint using various regression models. *Mater Lett*. 2022;325:132879.

doi: 10.1016/j.matlet.2022.132879